Xiaoyu Zhao[1], Amir Rashid[1] and Sasan Dadbakhsh[1]

Influence of Contouring and depth of machining on tensile properties of Inconel 625 made by Electron Beam Melting

Abstract

This research is to evaluate the manufacturability and to characterize the performance of Inconel 625 (IN625) by electron beam melting (EBM). After further modifying the commercial EBM parameters for Inconel 718, such as speed function for hatching and the line offset for both hatching and multi-beam contouring, nearly full dense samples (over 99.7% of the wrought material) are produced. It is shown that no contouring strategy generates a relatively rougher surface (approximately 29% in average) compared to the samples printed with contour, requiring even a further post-process machining. Furthermore, the microhardness after EBM is comparable to as-rolled and annealed IN625 material. The samples machined from bulk specimens exhibit good tensile properties regardless of the contouring strategy due to the high depth of machining (5.5mm). However, for the near-net shaped specimens with only 2.1 mm machining of the surfaces, elongation is significantly affected by the contouring strategy. This is in such a manner that the contoured near-net shape parts show relatively 32% less elongation compared to the samples without any contour. Accordingly, multi-beam contouring is better to be avoided to reach tensile properties comparable to the wrought material after a shallow machining, despite the fact that it can lead to a relative smoother surface finish after EBM.

Keywords

Additive Manufacturing, Electron Beam Melting, Inconel 625, Near-net Shape, Mechanical Properties

1. Introduction

Electron Beam Melting (EBM) is a powder-bed fusion process which creates products layer by layer based on sliced 3D models. Materials have been limitedly developed for EBM process. Amongst, Ti-6Al-4V has been thoroughly investigated while Inconel superalloys are in the fast explorative phase. Due to the necessity of post machining process, most researchers play safe and utilise a very deep machining before their mechanical evaluations, as we call it use of bulk products for reporting the material properties.

As mentioned, the bulk samples are widely used for investigating the capability of the EBM process. For example, many researchers [1]–[3] have evaluated the influence of different locations, building heights and orientations. The results indicated that the mechanical properties were not constant. This was attributed to the complex thermal history from this process that can impose different microstructures and even phases at different heights, locations and orientations.

In addition to the above-mentioned reports on the bulk samples, there are rare investigations to evaluate the mechanical properties of net-shaped components (mainly for Ti-

Department of Production Engineering, KTH Royal Institute of Technology

6Al-4V), i.e., those that are as-EBM and not machined. For example, Koike et al [4] compared the tensile properties between the as fabricated net shaped Ti-6Al-4V EBM parts, with cast and bulk EBM made samples. They have found that the bulk EBM and cast specimens exhibited a slightly higher ultimate tensile strength (UTS) and elongation compared to the net shape EBM parts. This was attributed to the rippled as-EBM surfaces and the higher oxygen content in their powder [4]. Moreover, Vayssette et al [5] reported that the samples with large surface roughness had a lower fatigue strength than the machined Ti-6Al-4V samples due to the crack initiation sites at the surface. They also suggested that the post-processing operations should be performed to improve the surface and hence the fatigue properties before the application.

Consequently, the contouring process is very important in EBM for the as fabricated surface. As default process parameters from Arcam, the contours are fabricated using a multi-spot function strategy, which is applied with higher linear beam energy density. As a result, the microstructure is different within the contouring and hatching regions, which can potentially influence the mechanical properties. This influence has been investigated in some other works for Inconel 718 [6]–[8] reporting a finer microstructure and a weaker texture from the multi-beam strategy compared to the hatching regions.

Despite all the previous works, no study has been investigated the influence of the depth of machining for the mechanical properties of near net-shaped components, i.e., those that are shallow machined after EBM to only smoothen the rough outer surfaces. Therefore, this study is performed to fulfill this research gap to realize the effect of contouring when one manufactures near-net shaped samples. Thus, the bulk samples (to be machine ~5.5 mm) and near-net shaped samples (to be machined only ~2.1 mm) are fabricated from Inconel 625 (IN625) in the same batch. Multi-beam contouring and no contouring are employed to also investigate the effect of contouring on near net-shaped properties. These are followed by surface roughness, hardness, and tensile experiments to give a complete understanding on the effects of the depth of machining and the contouring strategy.

2. Experimental Procedure

The gas atomized powder (Inconel 625) was supplied by Sandvik (Sweden) with a nominal chemical composition, as shown in Table 1. In this study, the powder was spherical with a particle size distribution between 45 and 105 µm in diameter. Materialise Magics (Materialise NV, Belgium) was used to design the layout and generated the support structure, which can be seen in Fig. 1a. All the samples were fabricated by EBM using an Arcam A2X machine at 1025˚C with a filament voltage of 60 KV. The average linear electron beam energy of the contouring strategy was around 0.9 [J/mm] and 0.5 [J/mm] for outer and inner contour, respectively. And the linear energy density for the hatching strategy was about 0.2 [J/mm]. The process parameters were supplied by an external company, which were modified based on the default process parameters of IN718 materials from GE Additive Arcam EBM. The modified parameters were speed function and the line offset. The cubes (C1-C5), with a size of 20x20x20mm, were used to perform the density and hardness tests. Density was measured with Archimedes-method. The weighing liquid was deionized water. The Vickers micro hardness ($HV_{0.1}$) was measured (on polished surfaces) by Mitutoyo HM-200 using 100 g loading and 15 s holding time. Seven measurements were performed along the building direction (Z plane) as well as the top surface (X-Y plane). All the tensile testing specimens were designed based on standard ASTM E8/E8M – 09 [9], while the gripping parts were

adapted to the testing bench (Fig. 1b). The peak-to-valley roughness (Rt) of the as fabricated samples was measured by varying the focus of the objective using stereomicroscope, ZEISS Axio zoom v16 with camera/detector AxioCam IC and Objective PlanNeoFluar Z 2.3x [ZEISS, Germany]. The accuracy of the measured results was ± 2 µm. In total, fifteen measurements were performed on each un-machined tensile samples (N1-N12). Amongst these, 5 readings were from the bottom gripping part, 5 readings from the reduced section, and 5 readings from the top gripping part. The post machining work was carried out on the bulk samples B1-B12, and near-net shaped samples NM1-NM12 (see Fig. 1a). 5.5mm and 2.1 mm were machined off from the bulk and near-net shaped parts, respectively. For tensile testing, Materials testing 4505 machine (Zwick/ Roell) with pulling speed of 1mm/min was used.

Table 1 Nominal Chemical composition of IN625

Element	Ni	Cr	Nb +Ta	Mo	Co	Ti	Al	Mn	Si	C	P	S	Fe
Wt%	Bal.	20-23	3.15-4.15	8-10	1	0.4	0.4	0,5	0.5	0.1	0.015	0.015	5

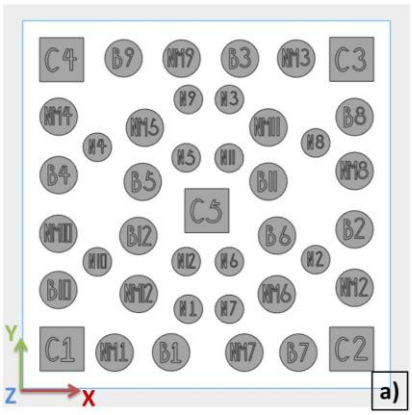

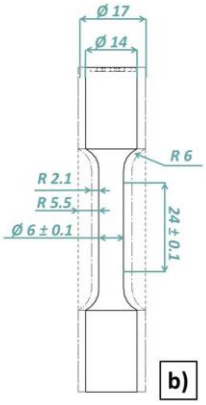

Sample Investigation Method	Density Cube	Tensile Specimens		
		Bulk Samples	Machined Near-net shaped Samples	Near-net Shaped Samples
Fabricated with Contour	C1-C2	B1-B6	NM1-NM6	N1-N6
Fabricated without Contour	C3-C5	B7-B12	NM7-NM12	N7-N12
Density	C1-C5			
Hardness	C1-C4			
Surface Roughness				N1-N12
Tensile Property		B1-B12	NM1-NM12	
Fracture Surface		B1-B12	NM1-NM12	

c)

Fig. 1: (a) Layout of the built, (b) dimension of the tensile specimens; dash, center, and solid lines represent the bulk, the near-net shaped, and the samples after machining respectively, and (c) summery of the coded samples.

3. Results

3.1. Density

Being consistent with the previously published results [10], the average density from all the 5 cubes was 8.432±0.013 g/cm^3. This means that the as fabricated samples achieved over 99.7% of the density of the wrought material (8.44 g/cm^3) [11]. This showed that the currently used processing parameters can lead to dense and nearly dense components from Inconel 625.

3.2. Hardness

The average of microhardness values ($HV_{0.1}$) was reported in Table 2. As seen, for the current samples, there was no large hardness difference between different locations. However, the measured hardness was much lower than the previously reported values [10] (about 250-280 HV for vertical and horizontal plans). This is while the current samples showed a hardness similar to the HIPed samples (which were reported to be about 210-220 HV for vertical and horizontal planes) [10]. The differences can attribute to the differences in the chemical composition of the powders and the EBM process parameters.

Table 2 Average HV values of the density cubes

Average hardness [$HV_{0.1}$]	Average on vertical (Z) Plane	Top (Random)
Cube 1	216.7±8.0	226.4±5.2
Cube 2	221.0±9.7	225.8±10.2
Cube 3	222.7±9.5	227.6±7.4
Cube 4	218.0±7.4	226.1±4.0
Overall Average	219.6±8.8	226.5±6.7

3.2. Surface Roughness

As shown in Table 3, on each sample, the roughness was varied at different locations, despite there was no clear trend of the roughness variation. The significant difference on surface roughness can be obtained between samples with and without contour. This is in such a manner that the samples without contour are in average about 29% rougher than the corresponding specimens with contour. Fig. 2 presents the surface of the as-built EBM samples with contour (Fig. 2a) and without contour (Fig. 2b) comparatively. In agreement with Table 2, the surface of the part without contouring (Fig. 2b) possessed more sintered peaks inherited from the EBM process.

Table 3 Summery of the surface roughness (Rt) measurement. Sample N1-N6 were EBMed with contour, while sample N7-N12 were EBMed without contour.

Sample with contour	Roughness /µm		Average/ µm	Sample without contour	Roughness /µm		Average/ µm	Position
N1	**Top**	157.2±28.3	158.5 ± 29.7	**N7**	**Top**	252.0±47.9	270.5 ± 48.8	Outside, left
	Reduced	150.2±30.8			**Reduced**	303.6±51.2		
	Bottom	168.2±33.7			**Bottom**	255.8±37.0		
N2	**Top**	177.8±29.5	162.0 ± 47.4	**N8**	**Top**	365.2±81.0	291.0 ± 77.3	Outside, right
	Reduced	139.6±60.8			**Reduced**	266.4±44.2		
	Bottom	168.6±47.8			**Bottom**	241.4±41.0		
N3	**Top**	159.2±40.1	200.3 ± 62.7	**N9**	**Top**	279.8±35.8	262.3 ± 36.2	Inside, right
	Reduced	268.0±41.2			**Reduced**	271.2±29.6		
	Bottom	167.2±44.4			**Bottom**	236.0±32.9		
N4	**Top**	231.8±64.0	230.3 ± 59.3	**N10**	**Top**	334.6±73.8	325.1 ± 61.3	Inside, left
	Reduced	252.8±54.8			**Reduced**	318.6±64.3		
	Bottom	206.4±62.2			**Bottom**	322.2±58.4		
N5	**Top**	195.2±61.9	213.4 ± 59.7	**N11**	**Top**	361.6±59.5	309.0± 61.6	Center, left
	Reduced	244.2±63.0			**Reduced**	293.8±28.0		
	Bottom	200.8±53.5			**Bottom**	271.6±58.9		
N6	**Top**	265.4±32.6	254.3 ± 47.6	**N12**	**Top**	263.6±44.1	256.3 ± 51.9	Center, right
	Reduced	287.0±48.3			**Reduced**	284.4±65.3		
	Bottom	210.4±25.5			**Bottom**	220.8±24.4		
Total Average with contour			202.8±61.8	**Total Average without contour**			285.7±61.4	

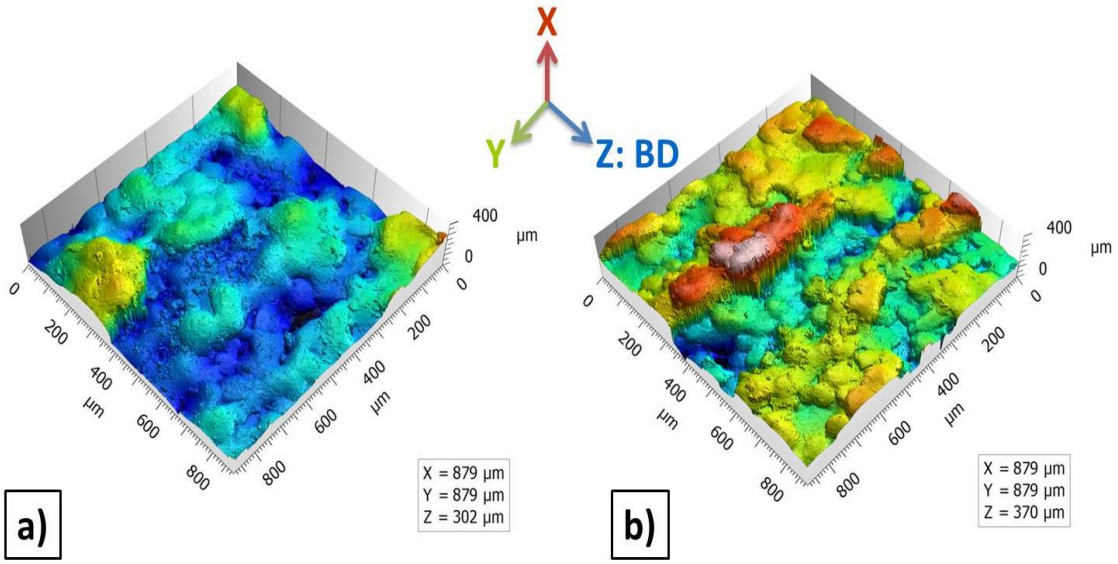

Fig. 2 The surfaces of a) sample C1 with contour and b) sample C4 without any contour.

3.4. Tensile Property

In this study, the tensile properties of all the samples fulfilled the requirements of ASTM F3056– 14 standard for powder bed fusion of IN625, i.e., YS = 275MPa, UTS = 485 MPa, and elongation to break =30% [12]. However, there are some differences among the samples fabricated with different conditions.

3.4.1. Bulk Sample

Fig. 3 demonstrates the tensile properties of bulk samples. Solid lines belong to the samples with contour (Fig. 3a) and in comparison the dash lines present the samples without contour (Fig. 3b). As seen, there is no clear difference between the parts with and without contours. This is since contouring influence has been removed due to deep machining (~ 5.5 mm). Overall, the average YS is 318.7±11.6 MPa, UTS is 635.6±19.7 MPa and elongation is 50.2±2.1%.

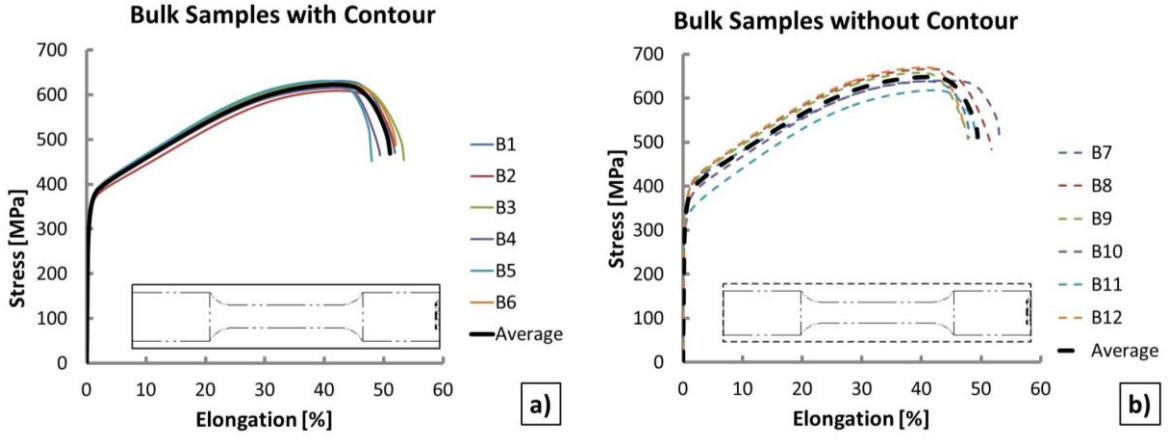

Fig. 3 Tensile properties of samples EBMed (a) with contour and (b) without contour and deeply machined from bulk cylinders.

3.4.2. Near-net shaped samples

The tensile properties of all the near-net shaped samples fulfilled the criteria of the standard. However, the samples fabricated with contour (Fig. 4a) demonstrated much lower elongation compared to the samples without contour (Fig. 4b) as well as the samples from the bulk material (Fig. 3). The average values of samples with contour are 333.6±12.9 MPa for YS, 634.5±20.7 MPa for UTS, and 34.5±4.2% for elongation. The average YS and UTS of samples without contour are 329±8.4MPa and 652.5±17.5MPa, and Elongation of 50.0±3.5%. It means that contouring, even after 2.1 mm machining, has reduced the elongation relatively around 32% (i.e., ~ (60.8 - 41.1)/60.8).

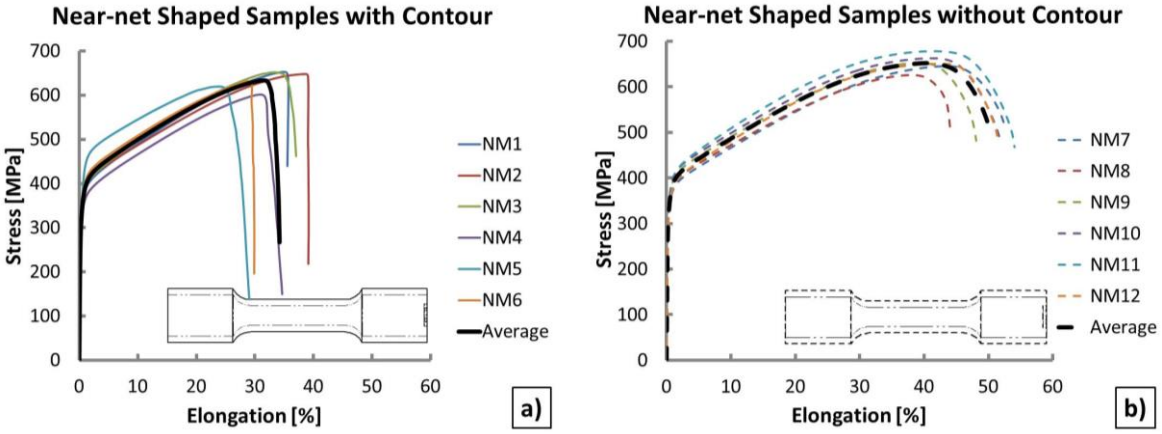

Fig. 4 Tensile properties of samples printed (a) with contour and (b) without contour and machined from near-net shaped samples.

3.5. Fracture Surface Analysis

Fig. 5 presents the fracture surface of the bulk samples. Obvious necking and deep/severe cracks (especially within central regions) were observed in the bulk samples printed with contour (B1-B6), as shown in Fig. 5a-c. Likewise, the samples without contour (B7-B12) showed similar ductile fracture surfaces (Fig. 5d-f)). This similar behavior can be attributed to the high depth of machining (~5.5 mm).

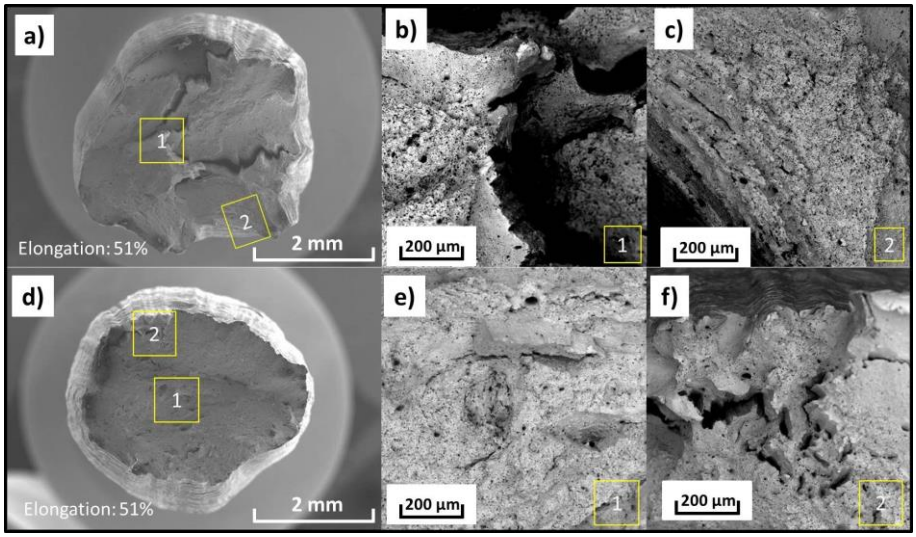

Fig. 5 Typical fracture surfaces of bulk samples; With Contour: a), fracture surface; b), location 1; c), location 2. Without Contour: d), fracture surface; e), location 1; f), location 2

In contrast, Fig. 6 shows the fracture surfaces of the near-net shaped specimens. As seen, the deformation seems to be less severe compared to the bulk samples (see Fig. 5). Nevertheless, necking seems to have proceeded further for the near-net shaped parts without contouring (compare Fig. 6d to Fig. 6a). This could be a demonstration for more ductility of the samples that were produced without any contour. Focusing on the near-net shaped samples with contour, one may also identify a higher number of tiny pores within the border region compare to the central areas.

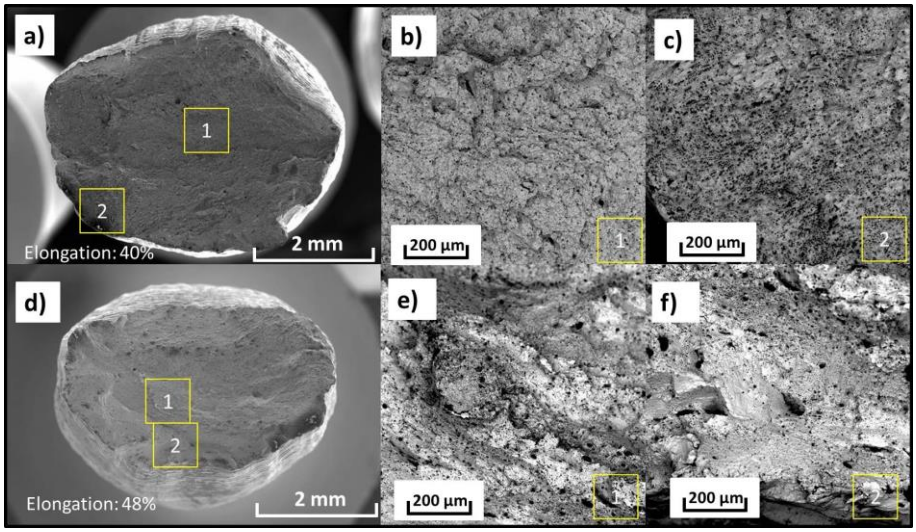

Fig. 6 Typical fracture surfaces of near-net shaped samples; With Contour: a), fracture surface; b), location 1; c), location 2. Without Contour: d), fracture surface; e), location 1; f), location 2

4. Discussion

According to the mentioned results, the used EBM parameters were able to successfully fabricate nearly full dense products with relative densities over 99.5%. The average Vickers hardness in this study is 219.6±8.8$HV_{0.1}$ which is inferior to the literature. The difference in hardness to the early publication must relate to the different applied process parameters. Since it is not possible to know what process parameters have been used for early publication, the microstructure analysis should be performed in order to analyze the differences between the samples from different research work.

Regarding the tensile properties (see Fig. 3-4), the YS, UTS, and elongation of the manufactured parts generally reached the requirements set by the standard ASTM F3056 – 14, as summarized in Table 4 [12]. Such satisfactory tensile properties led to a general appearance of cup-and-cone fractures. More specifically, all the bulk samples showed same behavior due to the high machining depth (~5.5 mm in radius) which removed all the superficial defects within contouring regions. In contrast, the significant differences can be observed between the near-net shaped samples with and without contour. As described, necking was less evident for the near net shaped part with contouring, as a result of a premature failure due to excess of the porosities around the border regions (compare Fig. 6c to Fig. 6b). Consequent to formation of tiny porosities due to the contouring, only near-net parts without contour could reach a ductility similar to the bulk samples (see Fig. 3-Fig. 4). The current findings are in agreement with the previous studies, as some researches have reported porosities around the border regions associated to the lack of fusion between powder particles [13].

As discussed, the contorting using a multi-beam strategy has a rather negative influence on the tensile elongation due to formation of more porosity at the contouring regions. Therefore, one may question why multi-beam strategy has been used in the first place. The answer is perhaps traceable within a higher production rate as well as the current surface roughness findings, as shown in Fig. 2. In fact, the samples with contour had relatively smoother surfaces (around 29% smoother in average) compared to the samples without contour. This can be attributed to the tiny melting pools (as dots) which were solidified and shrank quickly, leaving narrow gap between the powder bed and solid edges. This restricts the successive sintering of the powders to the edges, creating a rather smoother outer surface compared to only hatching strategy (see Fig. 2). Regarding the presence of multitude of porosities within the multi-beam contouring region, although the source is not very clear, it can be perhaps related to a suboptimal melting pool topology in conjunction with inadequate overlapping between the neighboring spots. Accordingly, the process parameters for contouring should be investigated and re-optimized to also mitigate the residual pores at the border regions besides providing a higher productivity and a better surface finish.

Table 4 Summery of the tensile properties

Bulk Sample	YS [MPa]	UTS [MPa]	Elongation to break [%]	Near-net Sample	YS [MPa]	UTS [MPa]	Elongation to break [%]	Contouring
B1	314	613	52	**NM1**	334	653	36	YES
B2	305	609	51	**NM2**	332	648	40	
B3	317	627	53	**NM3**	333	652	37	
B4	306	615	50	**NM4**	314	601	35	
B5	317	631	48	**NM5**	354	619	29	
B6	311	623	52	**NM6**	334	632	30	
B7	335	638	48	**NM7**	321	645	52	NO
B8	330	666	51	**NM8**	321	626	44	
B9	340	657	48	**NM9**	335	652	48	
B10	312	640	53	**NM10**	340	662	51	
B11	307	618	49	**NM11**	334	678	54	
B12	326	669	47	**NM12**	323	650	51	
ASTM	275	485	30		275	485	30	

5. Conclusion

This work has researched successful EBM of IN625 where the mechanical properties of the bulk and the near-net shaped samples were compared. After shallow and deep machining, all the samples showed good and acceptable properties. However, there were some differences according to the employed contouring strategy, as below:

- The samples deeply machined from the bulk cylinders, whether with or without contouring process, showed similar mechanical behavior due to no remaining EBM superficial effects. Both the tensile strengths and elongations well exceeded the standard.
- The near-net shaped samples with shallow machining but without contouring could achieve similar mechanical behavior to the bulk samples.
- The multi-beam contouring led to a lower elongation of the samples even after a shallow machining. This was attributed to the possible formation of defects such as porosities within the contouring regions.

- The multi-beam contouring however improved the surface roughness Rt by about 29 percent.

Acknowledgement

The authors acknowledge the financial support provided by Excellence in Production Research (XPRES) and the IN625 material supplied by Sandvik (Sweden).

References

[1] N. Hrabe and T. Quinn, Effects of processing on microstructure and mechanical properties of a titanium alloy (Ti–6Al–4V) fabricated using electron beam melting (EBM), Part 2: Energy input, orientation, and location, Mater. Sci. Eng. A (2013, Volume 273) p. 271-277

[2] P. Wang, M. L. S. Nai, W. J. Sin, and J. Wei, Effect of Building Height on Microstructure and Mechanical Properties of Big-Sized Ti-6Al-4V Plate Fabricated by Electron Beam Melting, 4th International Conference on Material Science and Engineering Technology, MATEC Web of Conferences ICMSET 2015, Singapore (2015, Volume 30) p. 02001(1-4)

[3] S.H. Sun, Y. Koizumi, S. Kurosu, Y.P. Li, H. Matsumoto, and A. Chiba, Build direction dependence of microstructure and high-temperature tensile property of Co-Cr-Mo alloy fabricated by electron beam melting, Acta Mater. (2014, Volume 64) p. 154–168

[4] M. Koike, K. Martinez, L. Guo, G. Chahine, R. Kovacevic, and T. Okabe, Evaluation of titanium alloy fabricated using electron beam melting system for dental applications, J. Mater. Process. Technol.(2011,Volume 211) p. 1400–1408

[5] B. Vayssette, N. Saintier, C. Brugger, M. Elmay, and E. Pessard, Surface roughness of Ti-6Al-4V parts obtained by SLM and EBM: Effect on the High Cycle Fatigue life, Procedia Eng. (2018, Volume 213) p. 89–97

[6] R.R. Dehoff, M.M. Kirka, F.A. List, K.A. Unocic, and W.J. Sames, Crystallographic texture engineering through novel melt strategies via electron beam melting: Inconel 718, Mater. Sci. Technol. (2015, Volume 31) p. 939–944

[7] E. Cakmak et al., Microstructural and micromechanical characterization of IN718 theta shaped specimens built with electron beam melting, Acta Mater.(2016, Volume 108) p. 161–175

[8] D. Deng, J. Saarimäki, H. Söderberg, R.L. Peng, H. Brodin, and J. Moverare, Microstructural characterization of as-manufactured and heat treated electron beam melted inconel 718, Materials Science And Technology Conference And Exhibition 2016, MS&T'16, Salt Lake City, Utah USA (2016, Volume 1) p. 105–112, 2016.

[9] ASTM E8/E8M − 13a Standard Test Methods for Tension Testing of Metallic Materials 1, ASTM International, West Conshohocken www.astm.org (2009) p. 1–27

[10] L.E. Murr et al., Microstructural architecture, microstructures, and mechanical properties for a nickel-base superalloy fabricated by electron beam melting, Metall. Mater. Trans. A Phys. Metall. Mater. Sci.(2011, Volume 42) p. 3491–3508

[11] Technical Bulletin, Inconel Alloy 625. Special Metals Corporation (2013, vol. 625) p. 1–28

[12] ASTM F3055 – 14 Standard Specification for Additive Manufacturing Nickel Alloy (UNS N06625) with Powder Bed Fusion. ASTM International, West Conshohocken www.astm.org (2015) p.1-8
[13] S. Tammas-Williams, H. Zhao, F. Léonard, F. Derguti, I. Todd, and P.B. Prangnell, XCT analysis of the influence of melt strategies on defect population in Ti-6Al-4V components manufactured by Selective Electron Beam Melting, Mater. Charact.(2015, Volume 102) p. 47–61